DEFENCE R&D DÉFENSE

# Application of Wigner Distribution for the Detection of Accelerating Low-Altitude Aircraft using HF Surface-Wave Radar

T. Thayaparan and A. Yasotharan



**Defence R&D Canada**
TECHNICAL REPORT
DREO TR 2002-033
March 2002

National Defence Défense nationale

Canada

# Application of Wigner Distribution for the detection of accelerating low-altitude aircraft using HF surface-wave radar

T. Thayaparan
Defence Research Establishment Ottawa

A. Yasotharan
Unique Broadband Systems

**Defence Research Establishment Ottawa**

Technical Report

DREO TR 2002-033

March 2002

Author

Thayananthan Thayaparan

Approved by

Maria Rey
Head, Surface Radar Section

Approved for release by

Gordon Marwood
Chief Scientist, Defence Research Establishment Ottawa

## Abstract

Real radar data has been analysed using the Fourier transform method and the type-III Wigner distribution. The results show that whenever the target was detectable by the Fourier transform method, the target was also detectable by the smoothed type-III Wigner distribution method. In the other trials, the target was not detectable by the Fourier transform method but it was detectable by the smoothed type-III Wigner distribution method to varying degrees of success. Based on the analysis of real radar data, we conclude that the smoothed type-III Wigner distribution provides a promising method of detecting accelerating targets. However, more work needs to be done to find an optimum smoothing method. It may turn out that different smoothing methods have to be used depending on the acceleration and the closeness of the target to the clutter region. Another important contribution of the present work is the use of the type-III Wigner distribution rather than the type-I Wigner distribution which has been used by many other researchers. When the type-I Wigner distribution is used, the range of unambiguously measurable normalized velocities is $\pi$. Moreover, targets that are $\pi$ radians away from the clutter region in the spectral domain will be masked by the clutter and cannot be detected. The type-III Wigner distribution helps us to overcome these problems. When the type-III Wigner distribution is used, the range of unambiguously measurable normalized velocities is $2\pi$, and target that are $\pi$ radians away from the clutter region can be detected.

## Résumé

Des données radar réelles ont été analysées au moyen de la méthode de la transformée de Fourier et de la distribution de Wigner de type-III. Les résultats montrent que, lorsque la cible était détectable par la méthode de la transformée de Fourier, elle l'était aussi par la méthode de distribution de Wigner de type-III lissée. Dans les autres essais, la cible n'éétait pas détectable par la méthode de la transformée de Fourier, mais elle l'était par la méthode de distribution de Wigner de type-III lissée avec divers degrés de succès. L'analyse des données radar réelles permet de conclure que la distribution de Wigner de type-III lissée constitue une méthode prometteuse de détection des cibles en accélération. Il faudra cependant mener d'autres travaux pour trouver une méthode de lissage optimale. Il se peut qu'il faille utiliser différentes méthodes de lissage selon l'accélération de la cible et sa proximité de la région de clutter. Une autre contribution importante des travaux en cours est l'utilisation de la distribution de Wigner de type-III de préférence à la distribution de Wigner de type-I, dont de nombreux autres chercheurs se sont servi. Lorsque la distribution de Wigner de type-I est utilisée, la fourchette des vitesses normalisées mesurables non ambiguës est $\pi$. En outre, les cibles à $\pi$ radians de la région de clutter dans le domaine spectral seront masquées par le clutter, d'où impossibilité de les détecter. La distribution de Wigner de type-III permet de surmonter ces problèmes. Lorsque la distribution de Wigner de type-III est utilisée, la fourchette des vitesses normalisées mesurables non ambiguës est $2\pi$, et les cibles à $\pi$ radians de la région de clutter peuvent être détectées.

# Executive summary

One of the central problems in High Frequency (HF) radar data is the analysis of a time series. The Fourier transform method, or Doppler processing method, has been generally used in HF radar to detect targets that are moving with constant radial acceleration. Examples of accelerating targets are manoeuvring aircrafts and missiles. Thayaparan and Yasotharan [1] show that there are limitations and shortcomings in the Fourier transform method to detect accelerating targets because of the phenomenon known as Doppler smearing. They show that when the target is constantly accelerating, the Fourier method may still be used to detect the target and estimate its median velocity, provided the acceleration is small enough in the sense to be described in this report. It is shown that for a given acceleration, the number of pulses cannot be increased indefinitely without resulting in catastrophic failure of the method. Conversely, for a given number of pulses, the acceleration cannot be arbitrarily large without resulting in catastrophic failure of the method. Thus the number of pulses and the acceleration have to be matched to achieve optimum performance [1].

Consequently, for the interpretation of radar data in terms of a changing frequency content, we need a representation of our data as a function of both time and frequency. The purpose of this report is therefore to stress the importance of alternative methods which have received little attention in the past, namely, the joint time-frequency representation of signals. In this report, we choose the Wigner distribution, together with a ambiguity function, as the basic tools, since both possess some important properties which make them very attractive for time-frequency signal analysis [2].

Real HF radar data has been analysed using the Fourier transform method and the type-III Wigner distribution. The results show that whenever the target was detectable by the Fourier transform method, the target was detectable also by the smoothed type-III Wigner distribution method. In the other trials the target was not detectable by the Fourier transform method but the target was detectable by the smoothed type-III Wigner distribution method to varying degrees of success. Based on the analysis of real radar data, we conclude that the smoothed type-III Wigner distribution provides a promising method of detecting accelerating targets. However, more work has to be done to find an optimum smoothing method. It may turn out that different smoothing methods have to be used depending on the acceleration and the closeness of the target to the clutter region. Another important contribution of the present work is the use of the type-III Wigner distribution rather than the type-I Wigner distribution which has been used by many other researchers. When the type-I Wigner distribution is used, the range of unambiguously measurable normalized velocities is $\pi$. Moreover, targets that are $\pi$ radians away from the clutter region in the spectral domain be masked by the clutter and cannot be detected. The type-III Wigner distribution helps us to overcome these problems. When the type-III Wigner distribution is used, the range of unambiguously measurable normalized velocities is $2\pi$, and target that are $\pi$ radians away from the clutter region can be detected.

T. Thayaparan, A. Yasotharan. 2002. Application of Wigner Distribution for the detection of accelerating low-altitude aircraft using HF surface-wave radar. DREO TR 2002-033. Defence Research Establishment Ottawa.

# Sommaire

Un des principaux problèmes éprouvé avec les données de radar haute fréquence (HF) est l'analyse d'une série chronologique. La méthode á transformée de Fourier, ou la méthode de traitement Doppler, a généralement été utilisée dans le radar HF pour la détection des cibles à accélération radiale constante. Les cibles présentant une accélération sont, par exemple, les aéronefs qui effectuent des manuvres et les missiles. Thayaparan et Yasotharan [1] montrent que la méthode à transformée de Fourier comporte des limites et des lacunes pour la détection des cibles à accélération, en raison du phénomène appelé la persistance Doppler. Ils montrent que dans le cas d'une cible à accélération constante, la méthode de Fourier peut encore être appliquée pour détecter la cible et estimer sa vitesse médiane, à condition que l'accélération soit assez faible dans le contexte du présent rapport. On montre que pour une accélération donnée, le nombre d'impulsions ne peut pas être augmenté indéfiniment sans qu'il en résulte un échec catastrophique de la méthode. Inversement, pour un nombre donné d'impulsions, l'accélération ne peut pas augmenter arbitrairement sans qu'il en résulte aussi un échec catastrophique de la méthode. Ainsi, le nombre d'impulsions et l'accélération doivent être adaptés pour permettre des performances optimales [1].

Par conséquent, pour interpréter les données radar du point de vue d'un contenu en fréquences variable, nous devons les représenter aussi bien en fonction du temps qu'en fonction de la fréquence. L'objet du présent rapport est donc de souligner l'importance des méthodes de rechange auxquelles on a accordé peu d'attention par le passé, notamment la représentation temps-fréquence combinée des signaux. Dans le rapport, nous choisissons la distribution de Wigner avec une fonction d'ambiguïté comme outil de base, étant donné que ces deux éléments offrent certaines propriétés importantes qui présentent un grand intérêt pour l'analyse temps-fréquence des signauxă[2].

Des données radar HF réelles ont été analysées au moyen de la méthode de la transformée de Fourier et de la distribution de Wigner de type-III. Les résultats montrent que, lorsque la cible était détectable par la méthode de la transformée de Fourier, elle l'était aussi par la méthode de distribution de Wigner de type-III lissée. Lors des autres essais, la cible n'était pas détectable par la méthode de la transformée de Fourier, mais elle l'était par la méthode de distribution de Wigner de type-III lissée avec divers degrés de succès. L'analyse des données radar réelles permet de conclure que la distribution de Wigner de type-III lissée constitue une méthode prometteuse de détection des cibles en accélération. Il faudra cependant mener d'autres travaux pour trouver une méthode de lissage optimale. Il se peut qu'il faille utiliser différentes méthodes de lissage selon l'accélération de la cible et sa proximité de la région de clutter. Une autre contribution importante des travaux en cours est l'utilisation de la distribution de Wigner de type-III de préférence à la distribution de Wigner de type-I, dont de nombreux autres chercheurs se sont servi. Lorsque la distribution de Wigner de type-I est utilisée, la fourchette des vitesses normalisées mesurables non ambiguës est $\pi$. En outre, les cibles à $\pi$ radians de la région de clutter dans le domaine spectral seront masquées par le clutter, d'où impossibilité de les détecter. La distribution de

Wigner de type-III permet de surmonter ces problèmes. Lorsque la distribution de Wigner de type-III est utilisée, la fourchette des vitesses normalisées mesurables non ambiguës est $2\pi$, et les cibles à $\pi$ radians de la région de clutter peuvent être détectées.

T. Thayaparan, A. Yasotharan. 2002. Application de la distribution de Wigner pour la détection d'aéronefs à basse altitude en accélération dotés de radar à ondes de surface HF. DREO TR 2002-033. Centre de Recherches pour la Défense Ottawa.

# Table of contents

# List of figures

This page intentionally left blank.

# 1. Introduction

The Fourier Transform is at the heart of a wide range of techniques that are used in HF radar data analysis and processing. Mapping the data into the temporal frequency domain is an effective way of recording the data such that their global characteristics can be assessed. However, the change of frequency content with time is one of the main features we observe in HF radar data. Because of this change of frequency content with time, radar signals belong to the class of non-stationary signals.

One of the central problems in High Frequency radar data is the analysis of a time series. The Fourier transform method, or Doppler processing method, has been generally used in HF radar to detect targets that are moving with constant radial acceleration. Examples of accelerating targets are manoeuvring aircraft and missiles. Thayaparan and Yasotharan [1] show that there are limitations and shortcomings in the Fourier transform method to detect accelerating targets because of the phenomenon known as Doppler smearing. They show that when the target is constantly accelerating, the Fourier method may still be used to detect the target and estimate its median velocity, provided the acceleration is small enough in the sense to be described in the paper. It is shown that for a given acceleration, the number of pulses cannot be increased indefinitely without resulting in catastrophic failure of the method. Conversely, for a given number of pulses, the acceleration cannot be arbitrarily large without resulting in catastrophic failure of the method. Thus the number of pulses and the acceleration have to be matched to achieve optimum performance [1].

Consequently, for the interpretation of radar data in terms of a changing frequency content, we need a representation of our data as a function of both time and frequency. The purpose of this paper is therefore to stress the importance of alternative methods which have had little attention in the past, namely, the joint time-frequency representation of signals. In this report, we use the new discrete-time Wigner time-frequency distribution. This distribution was independently derived by the authors Thayananthan and Yasotharan [3]. But it had already been derived by Chan [4] in an effort to solve the problem of aliasing. Nevertheless, the optimality properties of this discrete-time Wigner distribution for signal detection were not observed in [4]. Therefore, in the context of signal detection, this discrete-time Wigner distribution seems new.

# 2. Signal Model

In this study, the radar is assumed to be of the Pulse Doppler type, that is, it sends out a uniform train of RF pulses and phase-coherently receives their returns. It is also assumes that the receiver has pulse compression capability so that a pulse return from an isolated target can be represented by a single sample of the compressed pulse.

## 2.1 Single-Target Scenario

Suppose the radar sends out $N$ pulses, one every $T$ seconds, and there is a target moving with constant radial acceleration. Assume that the range walk is negligible, that is, the change in range during the observation period of $NT$ seconds is negligible compared to the radar range resolution as determined by the width of the compressed pulse. Then the samples of the $N$ range-compressed pulses taken at the range of the target have the form

$$r(n) = s(n) + v(n), \qquad \text{for } n = 0, 1, 2, 3, \ldots, (N-1), \tag{1}$$

where

$$s(n) = a e^{j(b_0 + b_1 n + \frac{1}{2} b_2 n^2)}, \tag{2}$$

is the noise-free signal, and $v(n)$ is a sequence of independently and identically distributed (iid) samples of complex Gaussian noise with mean zero and variance $\sigma^2$.

The signal parameters $a$ and $b_0$ are the target amplitude and phase respectively. The signal parameters $b_1$ and $b_2$ are the normalized initial radial velocity and the normalized radial acceleration respectively.

### 2.1.1 Normalized Initial Velocity and Acceleration

The normalized initial radial velocity is defined as

$$b_1 = u\left(\frac{4\pi T}{\lambda}\right) \tag{3}$$

where $u$ is the initial radial velocity in meters/sec, $T$ is pulse repetition interval in secs, and $\lambda$ is the carrier wavelength in meters. Similarly, the normalized radial acceleration is defined as

$$b_2 = f\left(\frac{4\pi T^2}{\lambda}\right) \tag{4}$$

where $f$ is the radial acceleration in meters/sec/sec towards the radar. It can be seen that both of the above normalized quantities are non-dimensional.

To obtain these relations note that the increment in range $d$, measured from the beginning of the observation interval, as a function of continuous-time $t$, is $d(t) = ut + \frac{1}{2}ft^2$, and therefore the phase increment of a pulse as a function of discrete-time, or pulse index, is given by

$$2\pi\left(\frac{2d(nT)}{\lambda}\right) = \frac{4\pi}{\lambda}\left(unT + \frac{1}{2}fn^2T^2\right), \tag{5}$$

$$= u\left(\frac{4\pi T}{\lambda}\right)n + \frac{1}{2}f\left(\frac{4\pi T^2}{\lambda}\right)n^2. \tag{6}$$

In the rest of the discussion, the term *velocity* and *acceleration* refer to *normalized radial velocity* and *normalized radial acceleration* respectively.

### 2.1.2 Per-Pulse Signal-to-Noise Ratio

The Per-Pulse Signal-to-Noise Ratio is defined as

$$\mathrm{SNR}_{\mathrm{pulse}} = \left(\frac{a}{\sigma}\right)^2. \tag{7}$$

The performance measures of any detection method will depend on $\mathrm{SNR}_{\mathrm{pulse}}$ and the number of pulses $N$. The values of the signal parameters $b_1$ and $b_2$ may also influence performance. We are interested in detection methods whose performance will increase as $N$ increases regardless of the values of $b_1$ and $b_2$.

## 2.2 Multiple-Target Scenario - Targets Separated in Range

When there are multiple targets, as long as they are separated from one another in range by at least the radar range resolution as determined by the width of the compressed pulse, a model of the above form will be valid for each of them.

Thus, if there are two targets separated in range, the samples of the $N$ range-compressed pulses taken at the corresponding ranges of the targets have the form

(8) $r_1(n) = s_1(n) + v_1(n)$, and

(9) $r_2(n) = s_2(n) + v_2(n)$ for $n = 0, 1, 2, 3, \ldots, (N-1)$,

where $s_1(n)$ and $s_2(n)$ are the noise-free signals, and $v_1(n)$ and $v_2(n)$ are sequences of independently and identically distributed samples of complex Gaussian noise with mean zero and variance $\sigma^2$.

Because of the independence of $v_1(n)$ and $v_2(n)$, the model decouples into two single target models.

## 2.3 Multiple-Target Scenario - Targets Coincident in Range

When there are multiple targets coincident in range, the samples of the $N$ range-compressed pulses taken at the range of the targets have the form

(10) $r(n) = s(n) + v(n)$, for $n = 0, 1, 2, 3, \ldots, (N-1)$,

where $s(n)$ is the combined noise-free signal due to all targets and $v(n)$ is a sequence of independently and identically distributed samples of complex Gaussian noise with mean zero and variance $\sigma^2$. If there are $K$ targets, the combined noise-free signal has the form

(11) $$s(n) = \sum_{k=1}^{K} a_k e^{j(b_{k,0} + b_{k,1} n + \frac{1}{2} b_{k,2} n^2)},$$

where $a_k$ and $b_{k,0}$ are the amplitude and phase respectively of the $k^{\text{th}}$ target, and $b_{k,1}$ and $b_{k,2}$ are the normalized initial radial velocity and the normalized radial acceleration respectively of the $k^{\text{th}}$ target.

# 3. A Wigner Distribution Formulation for a Discrete-Time Chirp Signal

It is nearly 20 years ago that the Wigner distribution (also known as Wigner-Ville distribution) was given a prominent place in the signal processing community's spectrum of research interests. Recognition was given almost immediately for the potential of the Wigner distribution as a tool for displaying and analyzing signal characteristics in the time-frequency plane. This assessment was soundly supported by the long list of desirable mathematical properties, such as correct marginal and support properties, satisfied by the Wigner distribution. Unlike the spectrogram, for instance, the resolution of the Wigner distribution is not limited by the temporal or spectral properties of a window, since a window is not required in the definition of the Wigner distribution [3,5].

On the other hand, due to its high resolution and its quadratic nature, the Wigner distribution locally exhibits oscillations between positive and negative values to an extent that smoothing, in a certain sense in accordance with the Heisenberg uncertainty principle, is necessary to make it non-negative everywhere [6]. As a consequence, a pointwise interpretation of the Wigner distribution as a true probability density function is not possible. This circumstance has kept the discussions in the signal processing community quite animated, yielding all sorts of modified Wigner distributions through the design of smoothing kernels and distributions involving the signals in a non-quadratic way. Thus, to a large extent, the interest and research effort of the community has been directed at redefining and re-interpreting the Wigner distribution, with the purpose of obtaining a clear and useful display and analysis tool.

Besides being a useful display and analysis tool, the Wigner distribution can be a great help in the design of time-frequency filtering methods. In this section and the following sections, we develop such methods for the detection of aircraft from the noisy signals. The Wigner distribution was originally defined for continuous-time signals. A discrete-time version of it was proposed recently. Unfortunately, this discrete-time Wigner distribution suffers from aliasing effects, which prevent several of the properties of the continuous-time Wigner distribution from carrying over straightforwardly. In this report, a discrete-time Wigner distribution which does not suffer from aliasing is introduced. It is essentially an augmentation of the previous version, incorporating new information about the signal not contained in the previous version.

## 3.1 Three Definitions of Wigner Distribution for Discrete-Time Signals

Given a discrete-time signal $r(n)$, we consider three definitions of auto time-frequency distributions which have some properties analogous to those of the classical Wigner distribution defined for continuous-time signals [7].

It is straightforward to verify that these are real-valued functions.

### 3.1.1 Type-I Wigner Distribution

The type-I Wigner distribution $W_r^I(n,\theta)$ is defined as

$$W_r^I(n,\theta) = \sum_k r(n+k)r^*(n-k)e^{-j2k\theta}, \tag{12}$$

where $n$ is integer-valued and $\theta$ is real-valued. Note that this is the same as the definition provided in [7] except for the missing scaling factor 2 at the front.

It is easy to verify that the type-I Wigner distribution is a periodic function of $\theta$ with period $\pi$. This property are discussed more in the following subsections.

For a signal $r(n)$ that is zero outside $0 \leq n \leq (N-1)$, the type-I Wigner distribution is zero outside $0 \leq n \leq (N-1)$.

### 3.1.2 Type-II Wigner Distribution

The type-II Wigner distribution $W_r^{II}(n,\theta)$ is defined as

$$W_r^{II}(n,\theta) = \sum_k r(n+k+1)r^*(n-k)e^{-j(2k+1)\theta}, \tag{13}$$

where $n$ is integer-valued and $\theta$ is real-valued.

It is straight forward to verify that the type-II Wigner distribution is a periodic function of $\theta$ with period $2\pi$. It is also straight forward to verify that

$$W_r^{II}(n,\theta+\pi) = -W_r^{II}(n,\theta). \tag{14}$$

These properties are discussed more in the following subsections.

For a signal $r(n)$ that is zero outside $0 \leq n \leq (N-1)$, the type-II Wigner distribution is zero outside $0 \leq n \leq (N-2)$.

### 3.1.3 Type-III Wigner Distribution

The type-III Wigner distribution $W_r^{III}(n,\theta)$ is defined in terms of the type-I and type-II Wigner distributions as follows.

$$W_r^{III}(n,\theta) = \begin{cases} W_r^{I}(n/2,\theta) & \text{for even } n, \\ W_r^{II}((n-1)/2,\theta) & \text{for odd } n. \end{cases} \tag{15}$$

It is straight forward to verify that the type-III Wigner distribution is a periodic function of $\theta$ with period $2\pi$. This property is discussed more in the following subsections.

For a signal $r(m)$ that is zero outside $0 \leq m \leq (N-1)$, the the type-III Wigner distribution is zero outside $0 \leq n \leq 2(N-1)$. However, if we consider even $n$ to correspond to integer values of time and odd $n$ to correspond to half-integer values of time then the type-III Wigner distribution is zero outside the time range $0 \leq m \leq (N-1)$.

## 3.2 The Range of Unambiguously Measurable Velocities of the Type-I and Type-III Wigner Distribution Based Methods

As shown in Section 3.1.1, the period of the type-I Wigner distribution is $\pi$. Therefore the signals

$$ae^{j(b_0+b_1n+\frac{1}{2}b_2n^2)}, \text{ and} \tag{16}$$

$$ae^{j(\tilde{b}_0+(b_1+\pi)n+\frac{1}{2}b_2n^2)}, \tag{17}$$

gives rise to the same type-I Wigner distribution. In otherwords, if we detect, using the type-I Wigner distribution, the presence of a signal in the time-frequency plane with intercept and slope parameters $c_1$ and $c_2$ respectively, then we cannot resolve the ambiguity as to whether the physical signal was

$$ae^{j(c_0+c_1n+\frac{1}{2}c_2n^2)}, \text{ or} \tag{18}$$

$$ae^{j(c_0+(c_1+\pi)n+\frac{1}{2}c_2n^2)} \tag{19}$$

without external information.

In contrast, as shown in Section 3.1.3, the period of the type-III Wigner distribution is $2\pi$. Therefore the signals

(20) $$ae^{j(b_0+b_1n+\frac{1}{2}b_2n^2)}, \text{ and}$$

(21) $$ae^{j(\tilde{b}_0+(b_1+\pi)n+\frac{1}{2}b_2n^2)},$$

give rise to different type-III Wigner distributions.

If we detect, using the type-III Wigner distribution, the presence of a signal in the time-frequency plane with intercept and slope parameters $c_1$ and $c_2$ respectively, then there is no ambiguity as to whether the physical signal was

(22) $$ae^{j(c_0+c_1n+\frac{1}{2}c_2n^2)}, \text{ or}$$

(23) $$ae^{j(c_0+(c_1+\pi)n+\frac{1}{2}c_2n^2)}.$$

However we need external information to resolve the ambiguity as to whether the physical signal was

(24) $$ae^{j(c_0+c_1n+\frac{1}{2}c_2n^2)}, \text{ or}$$

(25) $$ae^{j(c_0+(c_1+2\pi)n+\frac{1}{2}c_2n^2)}.$$

## 3.3 The Wigner Distributions of the Discrete-Time Chirp Signal

In this sub-section we derive the type-I, type-II, and type-III Wigner distributions for the discrete-time chirp signal

(26) $$s(n) = ae^{j(b_0+b_1n+\frac{1}{2}b_2n^2)}, \text{ for } n = 0, 1, \ldots, (N-1),$$

defined in Section 2. These derivations have been done in Appendix A assuming $a = 1$. The results stated here are obtained by scaling those derived in the appendix by $a^2$. Note that the Wigner distributions do not depend on $b_0$.

### 3.3.1 The Type-I Wigner Distribution of $s(n)$

The Type-I Wigner Distribution $W_s^I(n,\theta)$ of $s(n)$ is given by

(27) $$W_s^I(n,\theta) = a^2 \begin{cases} 2\min(n, N-1-n)+1 & \text{if } \theta = b_1 + b_2 n \bmod \pi, \\ \frac{\sin[(\theta-(b_1+b_2n))(2\min(n,N-1-n)+1)]}{\sin[\theta-(b_1+b_2n)]} & \text{otherwise.} \end{cases}$$

for $0 \leq n \leq (N-1)$, and it is zero outside this range.

In a 3-dimensional plot [3], it has a ridge along the lines given by

$$\theta = b_1 + b_2 n \bmod \pi. \tag{28}$$

The height of the ridge is given by

$$2\min(n, N-1-n) + 1. \tag{29}$$

### 3.3.2 The Type-II Wigner distribution of $s(n)$

The Type-II Wigner Distribution $W_s^{II}(n,\theta)$ of $s(n)$ is given by

$$W_s^{II}(n,\theta) = a^2 \begin{cases} 2\min(n, N-2-n) + 2 & \text{if } \theta = b_1 + \frac{1}{2}b_2 + b_2 n \bmod 2\pi, \\ -(2\min(n, N-2-n) + 2) & \text{if } \theta = \pi + b_1 + \frac{1}{2}b_2 + b_2 n \bmod 2\pi, \\ \frac{\sin\left[\left(\theta - (b_1 + \frac{1}{2}b_2 + b_2 n)\right)(2\min(n, N-2-n)+2)\right]}{\sin\left[\theta - (b_1 + \frac{1}{2}b_2 + b_2 n)\right]} & \text{otherwise.} \end{cases} \tag{30}$$

for $0 \leq n \leq (N-2)$, and it is zero outside this range.

In a 3-dimensional plot [3], it has a ridge along the lines given by

$$\theta = b_1 + \frac{1}{2}b_2 + b_2 n \bmod 2\pi. \tag{31}$$

The height of the ridge is given by

$$2\min(n, N-2-n) + 2. \tag{32}$$

In a 3-dimensional plot, it also has a valley along the lines given by

$$\theta = \pi + b_1 + \frac{1}{2}b_2 + b_2 n \bmod \pi. \tag{33}$$

The depth of the valley is given by

$$2\min(n, N-2-n) + 2. \tag{34}$$

### 3.3.3 The Type-III Wigner distribution of $s(n)$

The Type-III Wigner Distribution $W_s^{III}(n,\theta)$ of $s(n)$ is given by

$$W_s^{III}(n,\theta) = a^2 \begin{cases} 2\min(\frac{n}{2}, N-1-\frac{n}{2})+1 & \text{if } \theta = b_1 + \frac{1}{2}b_2 n \bmod 2\pi, \\ (-1)^n \left[2\min(\frac{n}{2}, N-1-\frac{n}{2})+1\right] & \text{if } \theta = \pi + b_1 + \frac{1}{2}b_2 n \bmod 2\pi, \\ \frac{\sin\left[(\theta-(b_1+\frac{1}{2}b_2 n))(2\min(\frac{n}{2}, N-1-\frac{n}{2})+1)\right]}{\sin\left[\theta-(b_1+\frac{1}{2}b_2 n)\right]} & \text{otherwise.} \end{cases} \tag{35}$$

for $0 \leq n \leq 2(N-1)$, and it is zero outside this range.

In a 3-dimensional plot [3], it has a ridge along the lines given by

$$\theta = b_1 + \frac{1}{2}b_2 n \bmod 2\pi. \tag{36}$$

The height of the ridge is given by

$$\min(n, 2(N-1)-n)+1. \tag{37}$$

In a 3-dimensional plot, it also has an oscillatory structure along the lines give by

$$\theta = \pi + b_1 + \frac{1}{2}b_2 n \bmod 2\pi. \tag{38}$$

The period of the oscillation is one unit and the amplitude of the oscillation is given by

$$\min(n, 2(N-1)-n)+1. \tag{39}$$

# 4. An Ambiguity Function Formulation for a Discrete-Time Chirp Signal

The inverse Fourier transform of the Wigner distribution is called the ambiguity function (AF). The Fourier transform maps the Wigner distribution auto-components to a region centered on the region of the AF plane, whereas it maps the oscillatory Wigner distribution cross-components away from the origin [8].

The fact that the auto- and cross-components are spatially separated in the AF domain means that if we apply mask function to the AF, we can suppress some of the cross-components. This masking operation defines a new time-frequency representation (TFR)

$$\text{TFR} = \text{Fourier transform}\{\text{AF} \cdot \text{Kernel}\} \tag{40}$$

with properties different from the Wigner distribution. The mask function is called the 'kernel' of the TFR. Since there are many possible 2-dimensional kernel functions, there exist many different TFRs for the same signal. The class of all TFRs obtained in this fashion is called Cohen's class. A more detailed description of the ambiguity function is given [8].

## 4.1 Three Definitions of Ambiguity Function for Discrete-Time Signals

Given a discrete-time signal $r(n)$, we consider three definitions of ambiguity function which are related, via a two-dimensional Fourier transformation, to the three definitions of Wigner distribution given in Section 3.1.

### 4.1.1 Type-I Ambiguity Function

The type-I ambiguity function $A_r^I(k,\alpha)$ is defined as

$$A_r^I(k,\alpha) = \sum_m r(m+k)r^*(m-k)e^{j2m\alpha}, \tag{41}$$

where $k$ is integer-valued and $\alpha$ is real-valued.

For a signal $r(n)$ that is zero outside $0 \le n \le (N-1)$, the type-I ambiguity function is zero outside $-\text{floor}\left(\frac{N-1}{2}\right) \le k \le \text{floor}\left(\frac{N-1}{2}\right)$.

### 4.1.2 Type-II Ambiguity Function

The type-II ambiguity function $A_r^{II}(k,\alpha)$ is defined as

$$A_r^{II}(k,\alpha) = \sum_m r(m+k+1)r^*(m-k)e^{j(2m+1)\alpha}, \tag{42}$$

where $k$ is integer-valued and $\alpha$ is real-valued.

For a signal $r(n)$ that is zero outside $0 \le n \le (N-1)$, the type-II ambiguity function is zero outside $-\text{floor}\left(\frac{N}{2}\right) \le k \le \text{floor}\left(\frac{N-2}{2}\right)$.

### 4.1.3 Type-III Ambiguity Function

The type-III ambiguity function $A_r^{III}(k,\alpha)$ is defined in terms of the type-I and type-II ambiguity functions as follows.

$$A_r^{III}(k,\alpha) = \begin{cases} A_r^{I}(k/2,\alpha) & \text{for even } k, \\ A_r^{II}((k-1)/2,\alpha) & \text{for odd } k. \end{cases} \tag{43}$$

For a signal $r(n)$ that is zero outside $0 \le n \le (N-1)$, the type-III ambiguity function is zero outside $-(N-1) \le k \le (N-1)$.

### 4.1.4 Cross Ambiguity Functions Between Two Discrete-Time Signals

Given discrete-time signals $x(n)$ and $y(n)$, we can define cross ambiguity functions as straightforward extensions of the definitions given above. Thus

$$A_{x,y}^{I}(k,\alpha) = \sum_m x(m+k)y^*(m-k)e^{j2m\alpha}, \tag{44}$$

$$A_{x,y}^{II}(k,\alpha) = \sum_m x(m+k+1)y^*(m-k)e^{j(2m+1)\alpha}, \tag{45}$$

$$A_{x,y}^{III}(k,\alpha) = \begin{cases} A_{x,y}^{I}(k/2,\alpha) & \text{for even } k, \\ A_{x,y}^{II}((k-1)/2,\alpha) & \text{for odd } k. \end{cases} \tag{46}$$

## 4.2 The Ambiguity Functions of a Discrete-Time Chirp Signal

In this sub-section we derive the type-I, type-II, and type-III ambiguity functions of the discrete-time chirp signal

$$s(n) = \begin{cases} e^{j(b_1 n + \frac{1}{2} b_2 n^2)} & \text{if } 0 \le n \le (N-1) \\ 0 & \text{otherwise.} \end{cases} \tag{47}$$

### 4.2.1 Type-I Ambiguity Function

Recall that the type-I ambiguity function $A_s^I(k,\alpha)$ is defined as

$$A_s^I(k,\alpha) = \sum_m s(m+k)s^*(m-k)e^{j2m\alpha}, \tag{48}$$

where $k$ is integer-valued and $\alpha$ is real-valued.

It is straight forward to see that the signal product term $s(m+k)s^*(m-k)$ is zero outside the ranges $-\text{floor}\left(\frac{N-1}{2}\right) \le k \le \text{floor}\left(\frac{N-1}{2}\right)$ and $\max(k,-k) \le m \le N-1-\max(k,-k)$.

Thus, for $-\text{floor}\left(\frac{N-1}{2}\right) \le k \le \text{floor}\left(\frac{N-1}{2}\right)$, we have

$$A_s^I(k,\alpha) = e^{j2b_1 k} \sum_{m=\max(k,-k)}^{N-1-\max(k,-k)} e^{j2(b_2 k+\alpha)m}, \tag{49}$$

which is a sum of a geometric series that can be evaluated as

$$A_s^I(k,\alpha) = \begin{cases} e^{j2b_1 k}(N - 2\max(k,-k)) & \text{if } b_2 k + \alpha = 0 \bmod \pi, \\ e^{j2b_1 k} e^{j[(b_2 k+\alpha)(N-1)]} \left( \frac{\sin[(b_2 k+\alpha)(N-2\max(k,-k))]}{\sin[(b_2 k+\alpha)]} \right) & \text{otherwise.} \end{cases} \tag{50}$$

### 4.2.2 Type-II Ambiguity Function

Recall that the type-II ambiguity function $A_s^{II}(k,\alpha)$ is defined as

$$A_s^{II}(k,\alpha) = \sum_m s(m+k+1)s^*(m-k)e^{j(2m+1)\alpha}, \tag{51}$$

where $k$ is integer-valued and $\alpha$ is real-valued.

It can be seen that the signal product term $s(m+k+1)s^*(m-k)$ is zero outside the ranges $-\text{floor}\left(\frac{N}{2}\right) \le k \le \text{floor}\left(\frac{N-2}{2}\right)$ and $\max(k,-(k+1)) \le m \le N-2-\max(k,-(k+1))$.

Thus, for $-\text{floor}\left(\frac{N}{2}\right) \le k \le \text{floor}\left(\frac{N-2}{2}\right)$, we have

$$A_s^{II}(k,\alpha) = e^{j(b_1+\frac{1}{2}b_2)(2k+1)}e^{j\alpha}\sum_{m=\max(k,-(k+1))}^{N-2-\max(k,-(k+1))} e^{j2(b_2(k+\frac{1}{2})+\alpha)m}, \tag{52}$$

which is a sum of a geometric series that can be evaluated as

$$A_s^{II}(k,\alpha) = \begin{cases} e^{j2b_1(k+\frac{1}{2})}(N-1-2\max(k,-(k+1))) \text{ if } b_2(k+\frac{1}{2})+\alpha = 0 \bmod 2\pi, \\ e^{j2b_1(k+\frac{1}{2})}e^{j[(b_2(k+\frac{1}{2})+\alpha)(N-1)]}\left(\frac{\sin\left[(b_2(k+\frac{1}{2})+\alpha)(N-1-2\max(k,-(k+1)))\right]}{\sin\left[(b_2(k+\frac{1}{2})+\alpha)\right]}\right) \text{ otherwis} \end{cases} \tag{53}$$

### 4.2.3 Type-III Ambiguity Function

Recall that the type-III ambiguity function $A_s^{III}(k,\alpha)$ is defined in terms of the type-I and type-II ambiguity functions as

$$A_s^{III}(k,\alpha) = \begin{cases} A_s^{I}(k/2,\alpha) & \text{for even } k, \\ A_s^{II}((k-1)/2,\alpha) & \text{for odd } k. \end{cases} \tag{54}$$

Thus for $-(N-1) \le k \le (N-1)$,

$$A_s^{III}(k,\alpha) = \begin{cases} e^{jb_1k}(N-\max(k,-k)) & \text{if } \frac{1}{2}b_2k+\alpha = 0 \bmod 2\pi \\ e^{jb_1k}e^{j[(\frac{1}{2}b_2k+\alpha)(N-1)]}\left(\frac{\sin\left[(\frac{1}{2}b_2k+\alpha)(N-\max(k,-k))\right]}{\sin\left[(\frac{1}{2}b_2k+\alpha)\right]}\right) & \text{otherwise.} \end{cases} \tag{55}$$

## 4.3 The Cross Ambiguity Functions of Two Discrete-Time Chirp Signals

In this sub-section we derive the type-I, type-II, and type-III cross ambiguity functions of the discrete-time chirp signals

$$x(n) = \begin{cases} e^{j(a_1 n + \frac{1}{2}a_2 n^2)} & \text{if } 0 \le n \le (N-1) \\ 0 & \text{otherwise.} \end{cases}, \tag{56}$$

$$y(n) = \begin{cases} e^{j(b_1 n + \frac{1}{2}b_2 n^2)} & \text{if } 0 \le n \le (N-1) \\ 0 & \text{otherwise.} \end{cases} \tag{57}$$

### 4.3.1 Type-I Cross Ambiguity Function

Recall that the type-I cross ambiguity function $A^I_{x,y}(k,\alpha)$ is defined as

$$A^I_{x,y}(k,\alpha) = \sum_m x(m+k)y^*(m-k)e^{j2m\alpha}, \tag{58}$$

where $k$ is integer-valued and $\alpha$ is real-valued.

It is straight forward to see that the signal product term $x(m+k)y^*(m-k)$ is zero outside the ranges $-\text{floor}\left(\frac{N-1}{2}\right) \le k \le \text{floor}\left(\frac{N-1}{2}\right)$ and $\max(k,-k) \le m \le N-1-\max(k,-k)$.

Defining

$$a_1 + b_1 = c_1, \tag{59}$$
$$a_2 + b_2 = c_2, \tag{60}$$
$$a_1 - b_1 = d_1, \tag{61}$$
$$a_2 - b_2 = d_2, \tag{62}$$

we can show

$$A^I_{x,y}(k,\alpha) = e^{j(c_1 k + \frac{1}{2}d_2 k^2)} \sum_{m=\max(k,-k)}^{N-1-\max(k,-k)} e^{j((d_1 + c_2 k + 2\alpha)m + \frac{1}{2}d_2 m^2)}, \tag{63}$$

for $-\text{floor}\left(\frac{N-1}{2}\right) \le k \le \text{floor}\left(\frac{N-1}{2}\right)$.

**Special Case $d_2 = 0$**

$$A^I_{x,y}(k,\alpha) = \begin{cases} e^{jc_1 k}(N - 2\max(k,-k)) \text{ if } d_1 + c_2 k + 2\alpha = 0 \bmod \pi, \\ e^{jc_1 k} e^{j[\frac{1}{2}(d_1+c_2 k+2\alpha)(N-1)]} \left( \frac{\sin\left[\frac{1}{2}(d_1+c_2 k+2\alpha)(N-2\max(k,-k))\right]}{\sin\left[\frac{1}{2}(d_1+c_2 k+2\alpha)\right]} \right) \text{ otherwise.} \end{cases}$$

(64)

Thus $\left|A^I_{x,y}(k,\alpha)\right|$ is concentrated along the line $d_1 + c_2 k + 2\alpha = 0$ and symmetrically spread about it with respect to $\alpha$. For a fixed $k$, the amount of spread with respect to $\alpha$ can be measured by $1/(N - 2\max(k,-k))$.

**The General Case**

Although it seems difficult to evaluate $A^I_{x,y}(k,\alpha)$ in the general case, by writing

$$A^I_{x,y}(k,\alpha) = e^{j(c_1 k + \frac{1}{2}d_2 k^2)} e^{j\left(\left(d_1+\frac{1}{2}d_2\left(\frac{N-1}{2}\right)+c_2 k+2\alpha\right)\left(\frac{N-1}{2}\right)\right)} \sum_{m=\max(k,-k)}^{N-1-\max(k,-k)} e^{j\left(\left(d_1+d_2\left(\frac{N-1}{2}\right)+c_2 k+2\alpha\right)\left(m-\left(\frac{N-1}{2}\right)\right)+\frac{1}{2}d_2\left(m-\left(\frac{N-1}{2}\right)\right)^2\right)},$$

(65)

we can see that $\left|A^I_{x,y}(k,\alpha)\right|$ is symmetrically spread about the line $d_1 + d_2\left(\frac{N-1}{2}\right) + c_2 k + 2\alpha = 0$ with respect to $\alpha$. For small $d_2$, $\left|A^I_{x,y}(k,\alpha)\right|$ is concentrated along the same line. For a fixed $k$, the amount of spread with respect to $\alpha$ will depend on both $(N - 2\max(k,-k))$ and $d_2$.

### 4.3.2 Type-II Cross Ambiguity Function

Recall that the type-II cross ambiguity function $A^{II}_{x,y}(k,\alpha)$ is defined as

$$A^{II}_{x,y}(k,\alpha) = \sum_m x(m+k+1)y^*(m-k)e^{j(2m+1)\alpha}, \tag{66}$$

where $k$ is integer-valued and $\alpha$ is real-valued.

It is straight forward to see that the signal product term $x(m+k+1)y^*(m-k)$ is zero outside the ranges $-\text{floor}\left(\frac{N}{2}\right) \le k \le \text{floor}\left(\frac{N-2}{2}\right)$ and $\max(k,-(k+1)) \le m \le N-2-\max(k,-(k+1))$.

Defining

$$a_1 + b_1 = c_1, \tag{67}$$

$$a_2 + b_2 = c_2, \tag{68}$$

$$a_1 - b_1 = d_1, \tag{69}$$

$$a_2 - b_2 = d_2, \tag{70}$$

we can show

$$A^{II}_{x,y}(k,\alpha) = e^{j(c_1(k+\frac{1}{2})+\frac{1}{2}d_2(k+\frac{1}{2})^2)} \sum_{m=\max(k,-(k+1))}^{N-2-\max(k,-(k+1))} e^{j((d_1+c_2(k+\frac{1}{2})+2\alpha)(m+\frac{1}{2})+\frac{1}{2}d_2(m+\frac{1}{2})^2)}, \tag{71}$$

for $-\text{floor}\left(\frac{N}{2}\right) \le k \le \text{floor}\left(\frac{N-2}{2}\right)$.

**Special Case $d_2 = 0$**

$$A^{II}_{x,y}(k,\alpha) = \begin{cases} e^{jc_1(k+\frac{1}{2})}(N-1-2\max(k,-(k+1))) \text{ if } d_1 + c_2(k+\frac{1}{2}) + 2\alpha = 0 \bmod \pi, \\ e^{jc_1(k+\frac{1}{2})} e^{j[\frac{1}{2}(d_1+c_2(k+\frac{1}{2})+2\alpha)(N-1)]} \left( \dfrac{\sin\left[\frac{1}{2}(d_1+c_2(k+\frac{1}{2})+2\alpha)(N-1-2\max(k,-(k+1)))\right]}{\sin\left[\frac{1}{2}(d_1+c_2(k+\frac{1}{2})+2\alpha)\right]} \right. \\ \text{otherwise.} \end{cases} \tag{72}$$

Thus $\left|A^{II}_{x,y}(k,\alpha)\right|$ is concentrated along the line $d_1 + c_2(k+\frac{1}{2}) + 2\alpha = 0$ and symmetrically spread about it with respect to $\alpha$. For a fixed $k$, the amount of spread with respect to $\alpha$ can be measured by $1/(N-1-2\max(k,-(k+1)))$.

**The General Case**

Although it seems difficult to evaluate $A^{II}_{x,y}(k,\alpha)$ in the general case, by writing

$$A^{II}_{x,y}(k,\alpha) = e^{j(c_1(k+\frac{1}{2})+\frac{1}{2}d_2(k+\frac{1}{2})^2)} e^{j\left(\left(d_1+\frac{1}{2}d_2\left(\frac{N-1}{2}\right)+c_2(k+\frac{1}{2})+2\alpha\right)\left(\frac{N-1}{2}\right)\right)} \sum_{m=\max(k,-(k+1))}^{N-2-\max(k,-(k+1))} e^{j\left(\left(d_1+d_2\left(\frac{N-1}{2}\right)+c_2(k+\frac{1}{2})+2\alpha\right)\left(m-\left(\frac{N-2}{2}\right)\right)+\frac{1}{2}d_2\left(m-\left(\frac{N-2}{2}\right)\right)^2\right)}, \tag{73}$$

we can see that $\left|A_{x,y}^{II}(k,\alpha)\right|$ is symmetrically spread about the line $d_1 + d_2\left(\frac{N-1}{2}\right) + c_2(k+\frac{1}{2}) + 2\alpha = 0$ with respect to $\alpha$. For small $d_2$, $\left|A_{x,y}^{II}(k,\alpha)\right|$ is concentrated along the same line. For a fixed $k$, the amount of spread with respect to $\alpha$ will depend on both $(N-1-2\max(k,-(k+1)))$ and $d_2$.

### 4.3.3 Type-III Cross Ambiguity Function

Recall that the type-III cross ambiguity function $A_{x,y}^{III}(k,\alpha)$ is defined in terms of the type-I and type-II cross ambiguity functions as

$$A_{x,y}^{III}(k,\alpha) = \begin{cases} A_{x,y}^{I}(k/2,\alpha) & \text{for even } k, \\ A_{x,y}^{II}((k-1)/2,\alpha) & \text{for odd } k. \end{cases} \tag{74}$$

By writing

$$A_{x,y}^{III}(k,\alpha) = e^{j(c_1(\frac{k}{2})+\frac{1}{2}d_2(\frac{k}{2})^2)} e^{j\left(\left(d_1+\frac{1}{2}d_2\left(\frac{N-1}{2}\right)+c_2(\frac{k}{2})+2\alpha\right)\left(\frac{N-1}{2}\right)\right)} \sum_{m=0}^{N-1-\max(k,-k)} e^{j\left(\left(d_1+d_2\left(\frac{N-1}{2}\right)+c_2(\frac{k}{2})+2\alpha\right)\left(m-\left(\frac{N-1-\max(k,-k)}{2}\right)\right)+\frac{1}{2}d_2\left(m-\left(\frac{N-1-\max(k,-k)}{2}\right)\right)^2\right)}, \tag{75}$$

we can see that $\left|A_{x,y}^{III}(k,\alpha)\right|$ is symmetrically spread about the line $d_1 + d_2\left(\frac{N-1}{2}\right) + c_2(\frac{k}{2}) + 2\alpha = 0$ with respect to $\alpha$. For small $d_2$, $\left|A_{x,y}^{III}(k,\alpha)\right|$ is concentrated along the same line. For a fixed $k$, the amount of spread with respect to $\alpha$ will depend on both $(N-\max(k,-k))$ and $d_2$.

**The Special Case $d_2 = 0$**

$$A_{x,y}^{III}(k,\alpha) = \begin{cases} e^{jc_1(\frac{k}{2})}(N-\max(k,-k)) \text{ if } d_1 + c_2(\frac{k}{2}) + 2\alpha = 0 \bmod \pi, \\ e^{jc_1(\frac{k}{2})} e^{j[\frac{1}{2}(d_1+c_2(\frac{k}{2})+2\alpha)(N-1)]} \left(\frac{\sin\left[\frac{1}{2}(d_1+c_2(\frac{k}{2})+2\alpha)(N-\max(k,-k))\right]}{\sin\left[\frac{1}{2}(d_1+c_2(\frac{k}{2})+2\alpha)\right]}\right) \text{ otherwise.} \end{cases} \tag{76}$$

Thus $\left|A_{x,y}^{III}(k,\alpha)\right|$ is concentrated along the line $d_1 + c_2(\frac{k}{2}) + 2\alpha = 0$ and symmetrically spread about it with respect to $\alpha$. For a fixed $k$, the amount of spread with respect to $\alpha$ can be measured by $1/(N-\max(k,-k))$.

# 5. Detecting Targets in Clutter using Smoothed Wigner Distributions

When the Wigner Distribution (WD) of a radar signal, collected by a pulse Doppler High Frequency Surface Wave Radar during the known presence of a target, are displayed, it is virtually impossible to 'see' the target as a distinct line in the time-frequency plane. This was due to the fact that the strength of the background against which the target had to be detected was much larger than the strength of the target, and the sidelobes of the WD of the background and those of the interaction between the background and the target were obscuring the target.

In general, the background against which targets must be detected by a radar will constitute clutter and noise. In the case of High Frequency Surface Wave Radar (HFSWR) used over the ocean, the clutter is due to Bragg scattering from the surface of the ocean [9]. This clutter can be adequately modeled for our purposes by two targets that are each moving with constant radial velocity. One target moves towards the radar and the other moves away from the radar, with the magnitudes of radial velocities being equal. These are called the approaching and receding Braggs. The real radar signal can thus be modeled by three target signals - two of which represent the Braggs - plus noise.

Recall that the WD of a sum of two signals contains cross-terms due to the interaction between the two signals [2]. In the case of two chirp signals, the cross-terms are of an oscillatory nature and located midway between the lines along which the auto-terms are concentrated. The strength of the cross-terms is proportional to the square root of the product of the strengths of the auto terms.

Approximately speaking, the WD of a real radar signal contains three auto-terms due to the Braggs and the target, three cross-terms due to the interactions between the Braggs themselves and the Braggs and the target, and the interactions of the Braggs and the target with the noise. In the vicinity of the auto-term due to the target, the contribution of the other terms are noise-like with amplitudes larger than that of the target's auto-term, thereby obscuring the target.

The target's auto-term can be made clearly visible as a line by smoothing the WD. This smoothing can be realized as a two-dimensional convolution operation. The problem is to choose an appropriate convolution kernel function. In the following sub-section, we present the heuristics of the derivation of a smoothing kernel that was successfully used on the real radar data.

The smoothed WD shows the target as a distinct line that can be detected via a generic line detection method. We propose taking slices at fixed times and doing a peak detection first. Once the target has been detected and a coarse estimation of its velocity made on at least two time slices, the results can be used to obtain the initial velocity and acceleration parameters of the target. The scope of this study was limited to finding an appropriate smoothing kernel. The software developed provides a good testbed for

further experimentation with different choices of kernel functions.

In the case of a Line-of-Sight (LOS) radar used over land, the clutter is due to reflections from the surface of the earth. This clutter can be adequately modeled for our purposes by a stationary target. The general principles outlined in this report for HFSWR can also be applied for an HFLOS (High Frequency Line-of-Sight) radar.

## 5.1 Heuristics of the Derivation of the Smoothing Kernal

To choose an appropriate kernel function we use our knowledge of the auto- and cross-ambiguity functions of chirp signals as described in the previous section and the fact that the ambiguity function is the two-dimensional Fourier transform of the WD. Since convolution of the WD with a kernel function is equivalent to multiplication of the AF by the two-dimensional Fourier transform of the kernel function, we can choose an appropriate kernel by studying the auto- and cross-ambiguity functions of chirp signals [8].

We start by making some observations on auto- and cross-ambiguity functions of chirp signals. Recall that the AF is a function of the variables time-offset and frequency-offset. In the following, when we refer to the slope and intersect of a line we associate time-offset with x-axis and normalized frequency-offset with y-axis.

- The auto-ambiguity function of a chirp signal is concentrated along a line through the origin, with slope = -0.5 × normalized acceleration.
- The cross-ambiguity function of two chirp signals with the same acceleration is concentrated along the line with intercept = -0.5 × difference in the normalized initial velocities, slope = -0.5 × normalized acceleration.
- The cross-ambiguity function of two chirp signals with differing accelerations is spread about the line with intercept = -0.5 × difference in the normalized median velocities, slope = -0.5 × average of the normalized accelerations. The spread is symmetric in the frequency offset dimension about the above line. For small enough difference in the acceleration, the cross-ambiguity function is concentrated along the above line. For large difference in the acceleration, the cross ambiguity function gets smeared in the frequency offset dimension much like the Fourier power spectrum of an accelerating target gets smeared when the acceleration is large.

Based on the above we can make the following observations on the AF of an HFSWR signal containing Braggs and one target:

- For targets with (magnitude) acceleration less than
  Bragg velocity/ NumPulsesPerCPI, the regions where the cross-terms between the Braggs are concentrated will not overlap with the region where the target's auto-term is concentrated.

- For targets with (magnitude) median velocity greater than 3 × Bragg velocity, the regions where the cross-terms between the Braggs and the target are concentrated will not overlap with the region where the target's auto-term is concentrated.

Therefore, for targets satisfying the above conditions on the acceleration and the median velocity, we can suppress all cross-terms while preserving the target's auto-term simply by setting the value of the AF to zero over the region

frequency-offset > Bragg velocity -
0.5× Bragg cross term region's width in the frequency-offset dimension.

After suppressing the cross-terms on the AF, we can take the two-dimensional Fourier transform to obtain a smoothed WD. A more detailed description and discussion of different methods are given in [8].

## 5.2 Analysis of Real Radar Data

Real HF radar data was analysed using the Fourier transform method and the type-III Wigner distribution method. The data had been collected by a Pulse Doppler High Frequency Surface Wave Radar that uses a 10-element linear receiving antenna array. The data had been collected during the known presence of a target. The radar carrier frequency is 5.672 MHz and the pulse repetition frequency is 9.17762 Hz. There are ten trails and each trial corresponds to a block of 256 pulses. The detailed description of the radar is given by Chan [9,10].

The results of our analysis are presented in Figures 1-20. The results for the type-III Wigner distribution of the time series containing the aircraft are compared simultaneously with the Fourier transform of the aircraft signal. The results show that whenever the target was detectable by the Fourier method, that is in trials 3, 4 and 8, the target was detectable also by the smoothed type-III Wigner distribution method. For the trials 3, 4 and 8, the aircraft is moving with a constant radial velocity. In the other trials, that is in trails 1, 2 and 5, the target was not detectable by the Fourier method but the target was detectable by the smoothed type-III Wigner distribution method to varying degrees of success. For the trials 1, 2 and 5, the aircraft is moving with a constant radial acceleration. Trails 1, 2 and 5 show that there are limitations and shortcomings to the Fourier transform method to detect accelerating targets because of the phenomenon known as Doppler smearing. On the other hand, the time-frequency analysis has the capability to detect the target, since its resolution abilities are not reduced in the presence of a Doppler signature.

An important contribution of the present work is the use of the type-III WD rather than the type-I WD which has been used by many other researchers. When the type-I WD is used, the range of unambiguously measurable normalized velocities is $\pi$. Moreover, targets that are $\pi$ radians away from the clutter region in the spectral domain will get masked by the clutter and cannot be detected. The type-III WD helps us to overcome these problems. When the type-III WD is used, the range of unambiguously measurable

normalized velocities is $2\pi$, and target that are $\pi$ radians away from the clutter region can be detected.

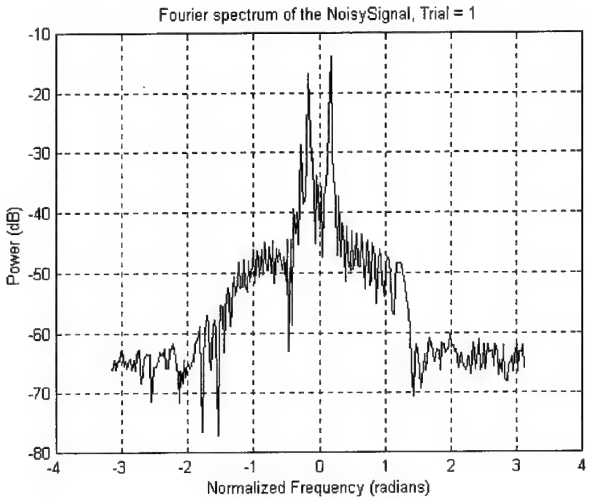


***Figure 1:*** *The Fourier transform of the aircraft signal.*

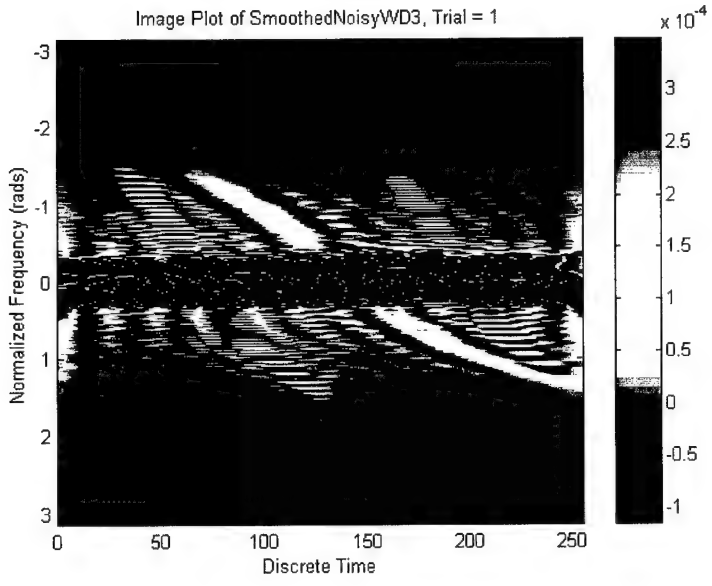


***Figure 2:*** *The type-III Wigner distribution of the time series containing the aircraft.*

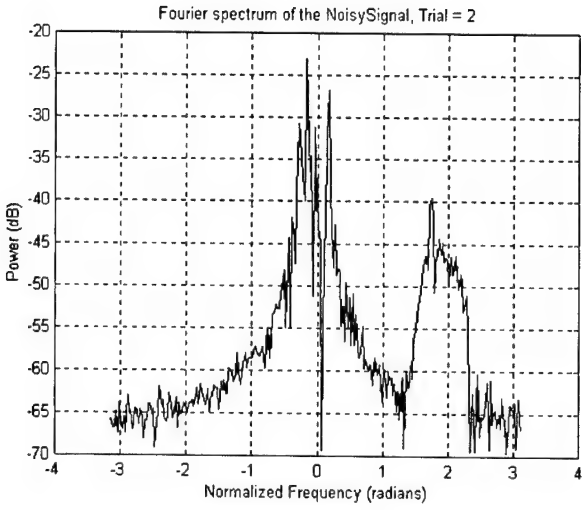


***Figure 3:*** *The Fourier transform of the aircraft signal.*

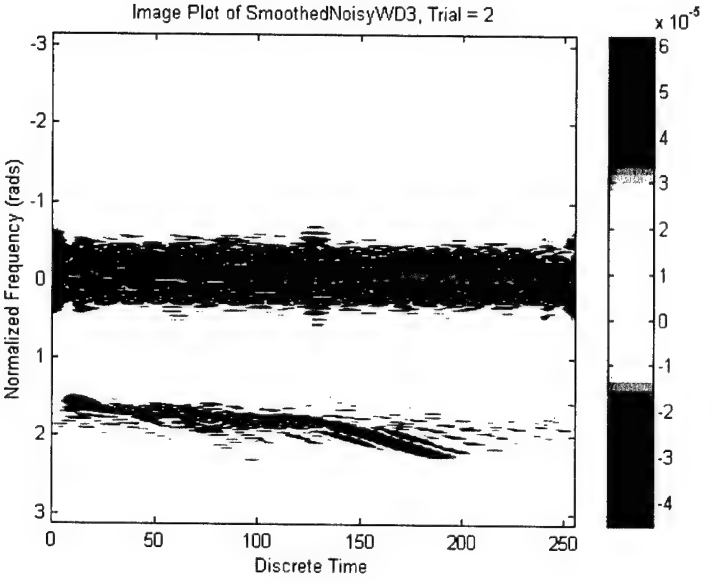


***Figure 4:*** *The type-III Wigner distribution of the time series containing the aircraft.*

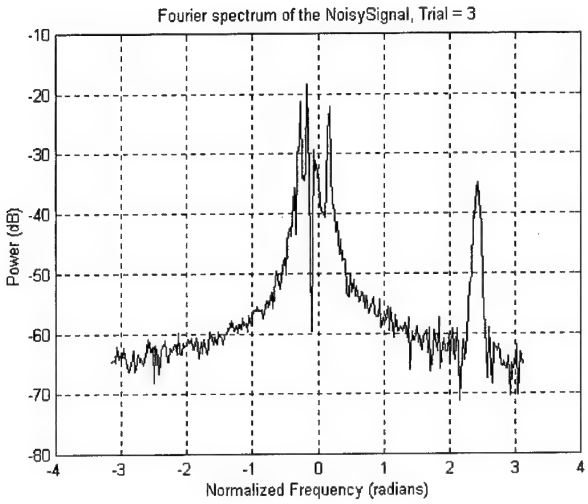


***Figure 5:*** *The Fourier transform of the aircraft signal.*

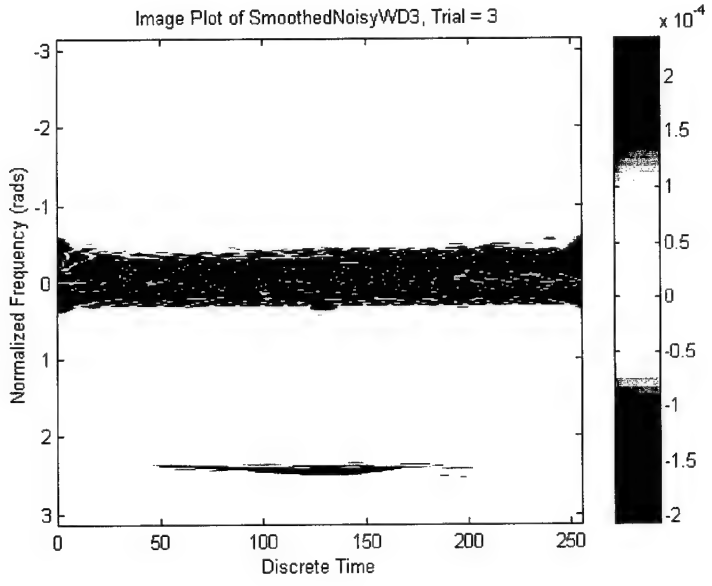


***Figure 6:*** *The type-III Wigner distribution of the time series containing the aircraft.*

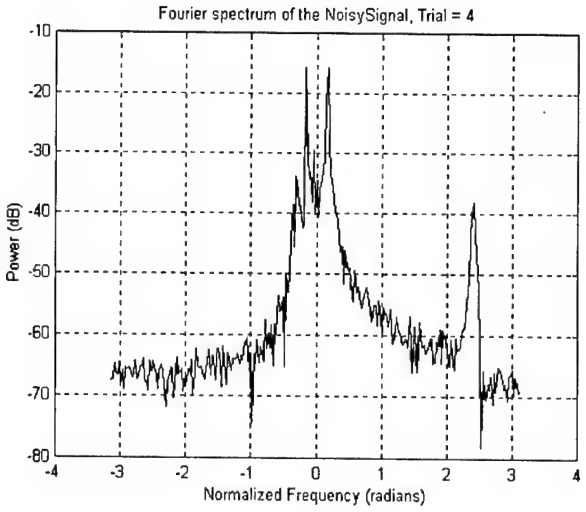


***Figure 7:*** *The Fourier transform of the aircraft signal.*

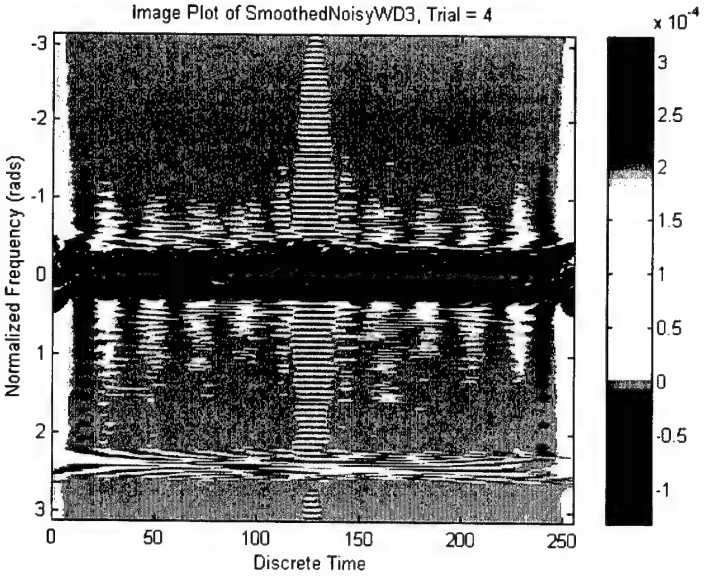


***Figure 8:*** *The type-III Wigner distribution of the time series containing the aircraft.*

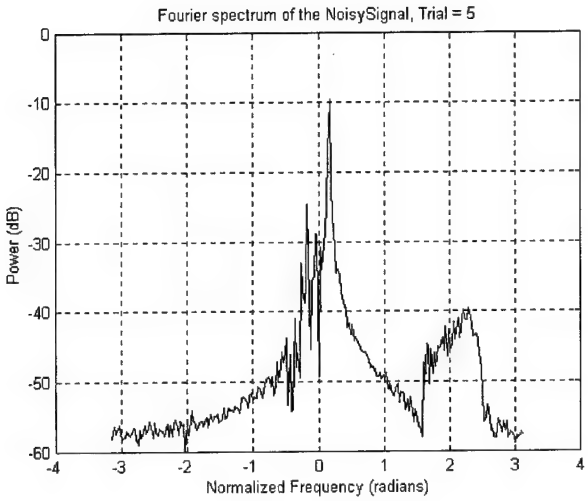


***Figure 9:*** *The Fourier transform of the aircraft signal.*

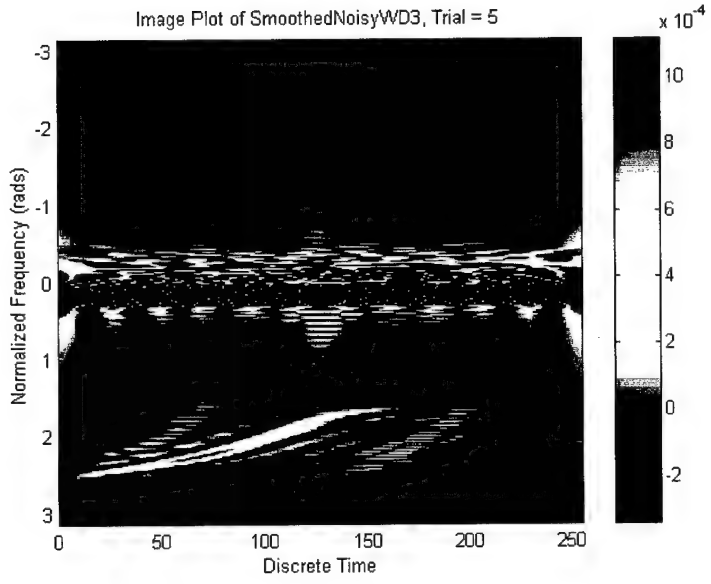


***Figure 10:*** *The type-III Wigner distribution of the time series containing the aircraft.*

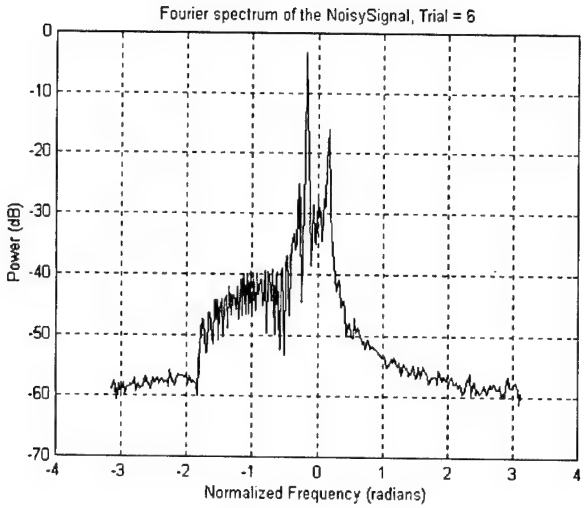


***Figure 11:*** *The Fourier transform of the aircraft signal.*

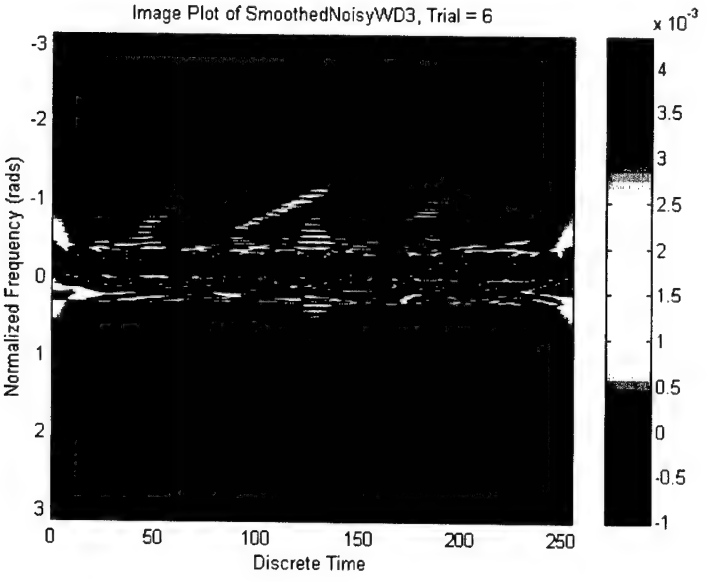


***Figure 12:*** *The type-III Wigner distribution of the time series containing the aircraft.*

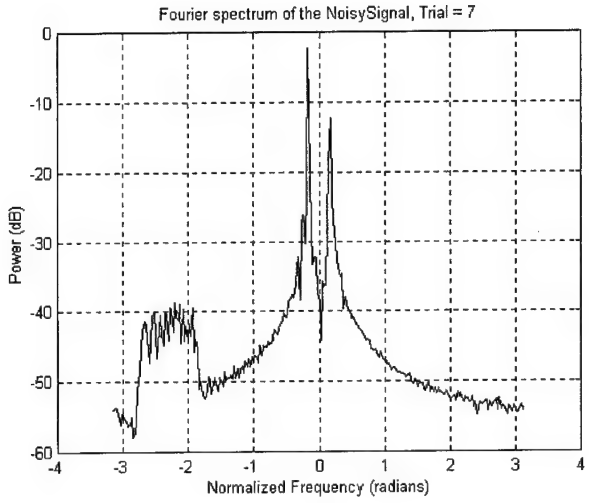


***Figure 13:*** *The Fourier transform of the aircraft signal.*

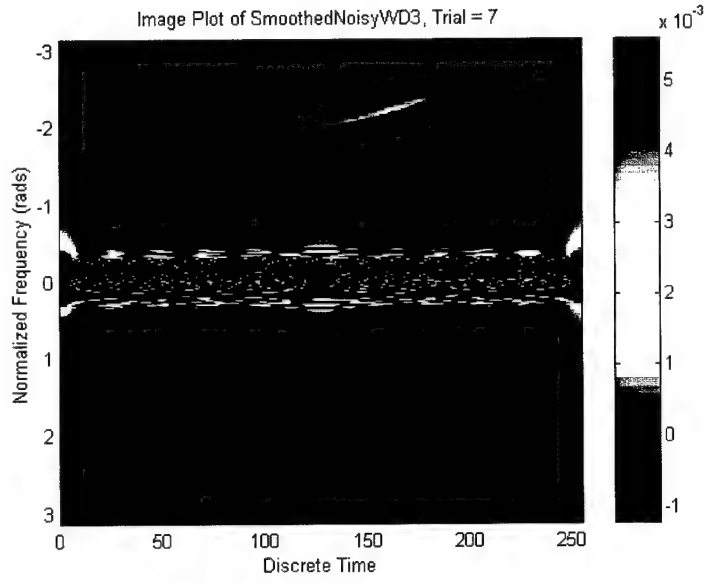


***Figure 14:*** *The type-III Wigner distribution of the time series containing the aircraft.*

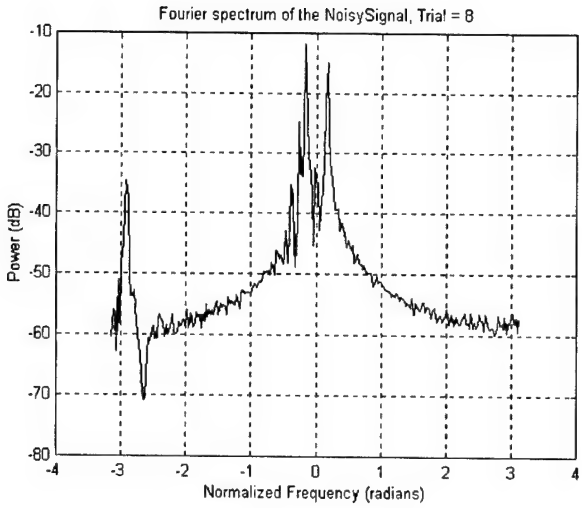


***Figure 15:*** *The Fourier transform of the aircraft signal.*

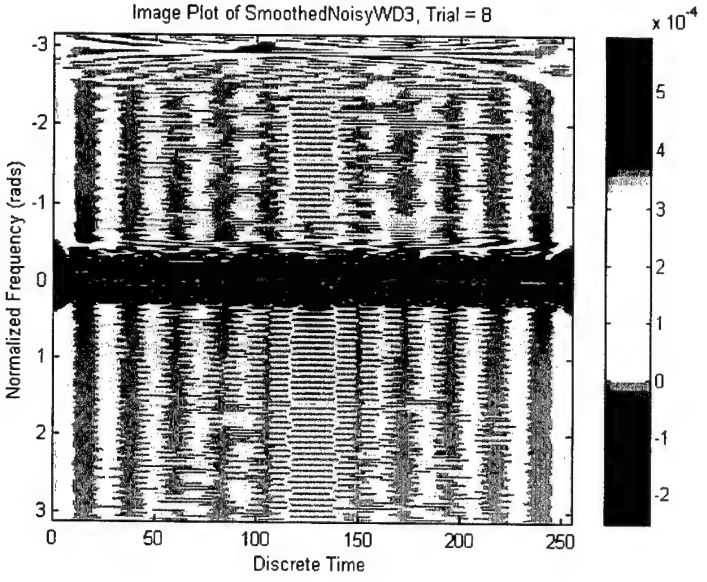


***Figure 16:*** *The type-III Wigner distribution of the time series containing the aircraft.*

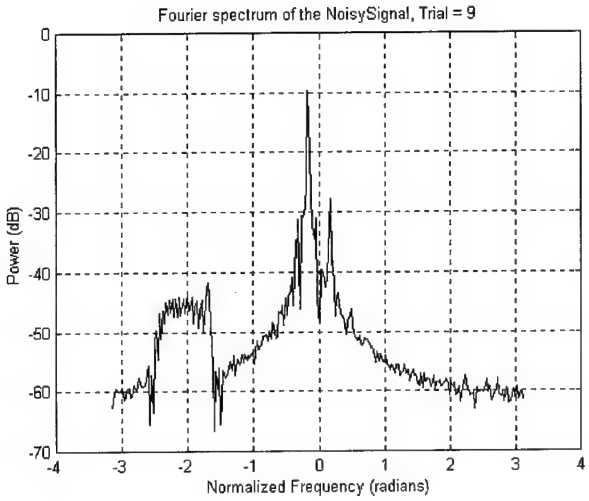


***Figure 17:*** *The Fourier transform of the aircraft signal.*

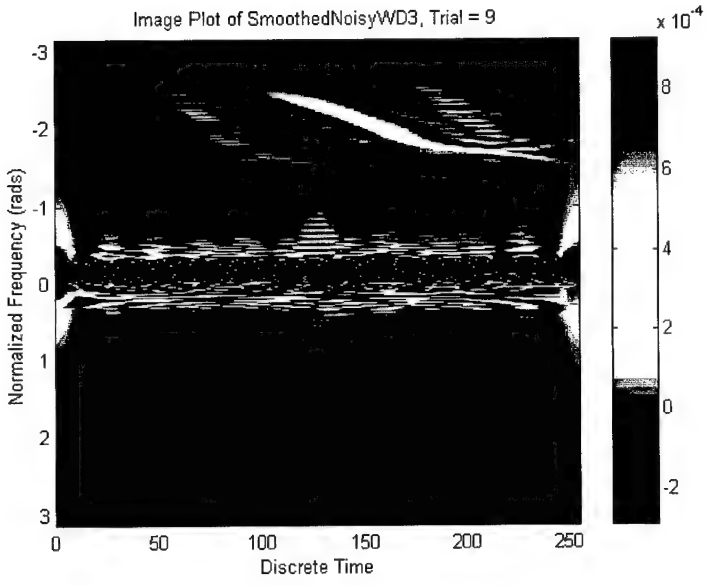


***Figure 18:*** *The type-III Wigner distribution of the time series containing the aircraft.*

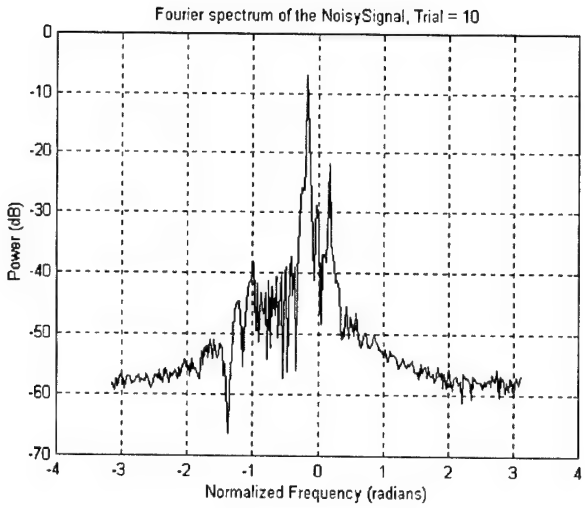


***Figure 19:*** *The Fourier transform of the aircraft signal.*

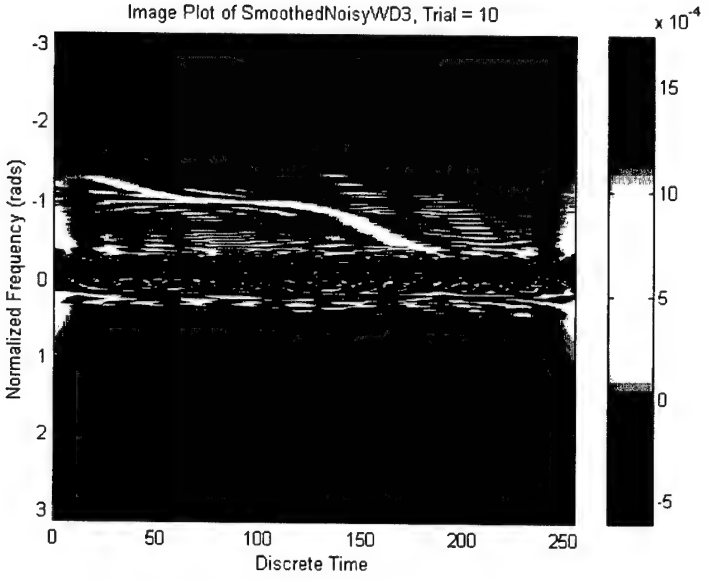


***Figure 20:*** *The type-III Wigner distribution of the time series containing the aircraft.*

# 6. Conclusion

This report examined the possibility of improving detection of low-altitude aircraft using High Frequency Surface Wave Radar. Because we are dealing with high speeds and accelerations, the time-frequency analysis has the capability to improve the detection, since its resolution abilities are not reduced in the presence of a spread Doppler signature.

The method involved use of the Wigner distribution, together with a ambiguity function. The results demonstrated superior performance for all cases considered. Although Wigner distribution has for a long time been known to possess interesting properties, its success in solving actual signal analysis problems has been limited. The Wigner distribution has been generally used as a signal interpretation tool only. The study has employed the Wigner distribution for solving a particularly challenging problem, demonstrating that use of time-frequency analysis can improve detection performance.

The results show that whenever the target was detectable by the Fourier transform method, the target was detectable also by the smoothed type-III Wigner distribution method. In the other trials the target was not detectable by the Fourier transform method but the target was detectable by the smoothed type-III Wigner distribution method to varying degrees of success.

Another important contribution of the present work is the use of the type-III Wigner distribution rather than the type-I Wigner distribution which has been used by many other researchers. When the type-I Wigner distribution is used, the range of unambiguously measurable normalized velocities is $\pi$. Moreover, targets that are $\pi$ radians away from the clutter region in the spectral domain will get masked by the clutter and cannot be detected. The type-III Wigner distribution helps us to overcome these problems. When the type-III Wigner distribution is used, the range of unambiguously measurable normalized velocities is $2\pi$, and target that are $\pi$ radians away from the clutter region can be detected.

# Annex A
# The Wigner Distributions of a Discrete-Time Chirp Signal

In this appendix we derive the type-I, type-II, and type-III Wigner distributions for the discrete-time chirp signal

$$s(n) = \begin{cases} e^{j(b_1 n + \frac{1}{2} b_2 n^2)} & \text{if } 0 \le n \le (N-1) \\ 0 & \text{otherwise.} \end{cases} \tag{A.1}$$

## A.1 Type-I Wigner Distribution

Recall that the type-I Wigner distribution $W_s^I(n,\theta)$ is defined as

$$W_s^I(n,\theta) = \sum_k s(n+k)s^*(n-k)e^{-j2k\theta}, \tag{A.2}$$

where $n$ is integer-valued and $\theta$ is real-valued.

It is easy to see that the signal product term $s(n+k)s^*(n-k)$ is zero outside the ranges $0 \le n \le (N-1)$ and $-\min(n, N-1-n) \le k \le \min(n, N-1-n)$. Thus $W_s^I(n,\theta) = 0$ outside $0 \le n \le (N-1)$.

Denote

$$l = \min(n, N-1-n) = \begin{cases} n & \text{if } n < (N-1)/2, \\ (N-1)/2 & \text{if } N \text{ is odd and } n = (N-1)/2, \\ N-1-n & \text{if } n > (N-1)/2. \end{cases} \tag{A.3}$$

In terms of this, for $0 \le n \le (N-1)$,

$$W_s^I(n,\theta) = \sum_{k=-l}^{l} e^{j(b_1(n+k)+\frac{1}{2}b_2(n+k)^2)} e^{-j(b_1(n-k)+\frac{1}{2}b_2(n-k)^2)} e^{-j2k\theta}, \tag{A.4}$$

$$= \sum_{k=-l}^{l} e^{j(b_1 2k + \frac{1}{2}b_2 4nk)} e^{-j2k\theta}, \tag{A.5}$$

$$= \sum_{k=-l}^{l} e^{-j(\theta-(b_1+b_2 n))2k}, \tag{A.6}$$

which is a sum of a geometric series that can be easily evaluated.

We first observe that the sum can be written as

$$\sum_{k=-l}^{l} e^{-j\alpha k}, \tag{A.7}$$

where $\alpha = 2(\theta - (b_1 + b_2 n))$ and then evaluate it to be

$$\sum_{k=-l}^{l} e^{-j\alpha k} = \begin{cases} 2l+1 & \text{if } \alpha = 0 \bmod 2\pi, \\ \frac{\sin\left[\alpha(l+\frac{1}{2})\right]}{\sin(\frac{\alpha}{2})} & \text{otherwise.} \end{cases} \tag{A.8}$$

Thus, for $0 \leq n \leq (N-1)$,

$$W_s^I(n,\theta) = \begin{cases} 2\min(n, N-1-n)+1 & \text{if } \theta = b_1 + b_2 n \bmod \pi, \\ \frac{\sin[(\theta-(b_1+b_2 n))(2\min(n,N-1-n)+1)]}{\sin[\theta-(b_1+b_2 n)]} & \text{otherwise.} \end{cases} \tag{A.9}$$

## A.2 Type-II Wigner Distribution

Recall that the type-II Wigner distribution $W_s^{II}(n,\theta)$ is defined as

$$W_s^{II}(n,\theta) = \sum_k s(n+k+1)s^*(n-k)e^{-j(2k+1)\theta}, \tag{A.10}$$

where $n$ is integer-valued and $\theta$ is real-valued.

It is easy to see that the signal product term $s(n+k+1)s^*(n-k)$ zero outside the ranges $0 \leq n \leq (N-2)$ and $-\min(n+1, N-1-n) \leq k \leq \min(n, N-2-n)$. Thus $W_s^{II}(n,\theta) = 0$ outside $0 \leq n \leq (N-2)$.

Denote

$$l = \min(n, N-2-n) = \begin{cases} n & \text{if } n < (N-2)/2, \\ (N-2)/2 & \text{if } N \text{ is even and } n = (N-2)/2, \\ N-2-n & \text{if } n > (N-2)/2. \end{cases} \tag{A.11}$$

In terms of this, for $0 \leq n \leq (N-2)$,

$$W_s^{II}(n,\theta) = \sum_{k=-(l+1)}^{l} e^{j(b_1(n+k+1)+\frac{1}{2}b_2(n+k+1)^2)} e^{-j(b_1(n-k)+\frac{1}{2}b_2(n-k)^2)} e^{-j(2k+1)\theta},$$

(A.12)

$$= \sum_{k=-(l+1)}^{l} e^{j(b_1(2k+1)+\frac{1}{2}b_2(4nk+2n+2k+1))} e^{-j(2k+1)\theta}, \quad \text{(A.13)}$$

$$= \sum_{k=-(l+1)}^{l} e^{-j(\theta-(b_1+\frac{1}{2}b_2+b_2n))(2k+1)}, \quad \text{(A.14)}$$

$$= e^{-j(\theta-(b_1+\frac{1}{2}b_2+b_2n))} \sum_{k=-(l+1)}^{l} e^{-j(\theta-(b_1+\frac{1}{2}b_2+b_2n))2k}, \quad \text{(A.15)}$$

which is a scaled version of a sum of a geometric series that can be easily evaluated.

We first observe that the sum can be written as

$$\sum_{k=-(l+1)}^{l} e^{-j\alpha k}, \quad \text{(A.16)}$$

where $\alpha = 2(\theta - (b_1 + \frac{1}{2}b_2 + b_2 n))$ and then evaluate it to be

$$\sum_{k=-(l+1)}^{l} e^{-j\alpha k} = \begin{cases} 2l+2 & \text{if } \alpha = 0 \bmod 2\pi, \\ e^{j\frac{\alpha}{2}} \left( \frac{\sin[\alpha(l+1)]}{\sin(\frac{\alpha}{2})} \right). \end{cases} \quad \text{(A.17)}$$

Now, introducing the scaling factor, we see that

$$e^{-j\frac{\alpha}{2}} \sum_{k=-(l+1)}^{l} e^{-j\alpha k} = \begin{cases} e^{-j\frac{\alpha}{2}}(2l+2) & \text{if } \alpha = 0 \bmod 2\pi, \\ \frac{\sin[\alpha(l+1)]}{\sin(\frac{\alpha}{2})}. \end{cases} \quad \text{(A.18)}$$

$$= \begin{cases} (2l+2) & \text{if } \frac{\alpha}{2} = 0 \bmod 2\pi, \\ -(2l+2) & \text{if } \frac{\alpha}{2} = \pi \bmod 2\pi, \\ \frac{\sin[\alpha(l+1)]}{\sin(\frac{\alpha}{2})}. \end{cases} \quad \text{(A.19)}$$

Thus, for $0 \leq n \leq (N-2)$,

$$W_s^{II}(n,\theta) = \begin{cases} 2\min(n, N-2-n)+2 & \text{if } \theta = b_1 + \frac{1}{2}b_2 + b_2 n \bmod 2\pi, \\ -(2\min(n, N-2-n)+2) & \text{if } \theta = \pi + b_1 + \frac{1}{2}b_2 + b_2 n \bmod 2\pi, \\ \frac{\sin\left[\left(\theta-(b_1+\frac{1}{2}b_2+b_2 n)\right)(2\min(n,N-2-n)+2)\right]}{\sin\left[\theta-(b_1+\frac{1}{2}b_2+b_2 n)\right]} & \text{otherwise.} \end{cases}$$

(A.20)

It is useful to write this as

$$W_s^{II}(n,\theta) = \begin{cases} 2\min(n+\frac{1}{2}, N-1-(n+\frac{1}{2}))+1 & \text{if } \theta = b_1 + b_2(n+\frac{1}{2}) \bmod 2\pi, \\ -\left[2\min(n+\frac{1}{2}, N-1-(n+\frac{1}{2}))+1\right] & \text{if } \theta = \pi + b_1 + b_2(n+\frac{1}{2}) \bmod 2\pi, \\ \frac{\sin\left[\left(\theta-(b_1+b_2(n+\frac{1}{2}))\right)\left(2\min(n+\frac{1}{2},N-1-(n+\frac{1}{2}))+1\right)\right]}{\sin\left[\theta-(b_1+b_2(n+\frac{1}{2}))\right]} & \text{otherwise.} \end{cases}$$

(A.21)

## A.3 Type-III Wigner Distribution

Recall that the type-III Wigner distribution $W_s^{III}(n,\theta)$ is defined in terms of the type-I and type-II Wigner distributions as

$$W_s^{III}(n,\theta) = \begin{cases} W_s^{I}(n/2,\theta) & \text{for even } n, \\ W_s^{II}((n-1)/2,\theta) & \text{for odd } n. \end{cases} \tag{A.22}$$

For $n$ even and $0 \le n \le 2(N-1)$,

$$W_s^{III}(n,\theta) = \begin{cases} 2\min(\frac{n}{2}, N-1-\frac{n}{2})+1 & \text{if } \theta = b_1 + \frac{1}{2}b_2 n \bmod \pi, \\ \frac{\sin\left[\left(\theta-(b_1+\frac{1}{2}b_2 n)\right)\left(2\min(\frac{n}{2},N-1-\frac{n}{2})+1\right)\right]}{\sin\left[\theta-(b_1+\frac{1}{2}b_2 n)\right]} & \text{otherwise.} \end{cases}$$

(A.23)

For $n$ odd and $0 \le n \le 2(N-1)$,

$$W_s^{III}(n,\theta) = \begin{cases} 2\min(\frac{n}{2}, N-1-\frac{n}{2})+1 & \text{if } \theta = b_1 + \frac{1}{2}b_2 n \bmod 2\pi, \\ -\left[2\min(\frac{n}{2}, N-1-\frac{n}{2})+1\right] & \text{if } \theta = \pi + b_1 + \frac{1}{2}b_2 n \bmod 2\pi, \\ \frac{\sin\left[\left(\theta-(b_1+\frac{1}{2}b_2 n)\right)\left(2\min(\frac{n}{2},N-1-\frac{n}{2})+1\right)\right]}{\sin\left[\theta-(b_1+\frac{1}{2}b_2 n)\right]} & \text{otherwise.} \end{cases}$$

(A.24)

Combining the above, for all $0 \le n \le 2(N-1)$,

$$W_s^{III}(n,\theta) = \begin{cases} 2\min(\frac{n}{2}, N-1-\frac{n}{2})+1 & \text{if } \theta = b_1 + \frac{1}{2}b_2 n \bmod 2\pi, \\ (-1)^n \left[2\min(\frac{n}{2}, N-1-\frac{n}{2})+1\right] & \text{if } \theta = \pi + b_1 + \frac{1}{2}b_2 n \bmod 2\pi, \\ \frac{\sin\left[\left(\theta-(b_1+\frac{1}{2}b_2 n)\right)\left(2\min(\frac{n}{2}, N-1-\frac{n}{2})+1\right)\right]}{\sin\left[\theta-(b_1+\frac{1}{2}b_2 n)\right]} & \text{otherwise.} \end{cases}$$

(A.25)

## References


1. Thayaparan, T. and Yasotharan, A. (2000). Limitations and Strengths of the Fourier transform method to detect accelerating targets, Defence Research Establishment Ottawa, *DREO TM 2000-078.*

2. Thayaparan, T. (2000). Linear and Quadratic time-frequency representations, Defence Research Establishment Ottawa, *DREO TM 2000-080.*

3. Thayaparan, T. and Yasotharan, A. (2001). A Novel approach for the Wigner distribution formulation of the optimum detection problem for a discrete-time chirp signal, Defence Research Establishment Ottawa, *DREO TM 2001-xxx.*

4. Chan, D. S. K. (1982). A Non-Aliased Discrete-Time Wigner Distribution for Time-Frequency Signal Analysis, *Proc. ICASSP '82,* 1333-1336.

5. Cohen, L. (1989). Time-frequency distributions - a review, *Proc. IEEE,* 77, 7, July.

6. Cohen, L. (1995). Time-frequency analysis, *Prentice Hall Signal Processing Series,* Prentice-Hall Inc., New Jersey.

7. Claasen, T. A. C. M. and Mecklenbrauker, W. F. G. (1980). The Wigner Distribution - A Tool for Time-Frequency Signal Analysis, Part-II: Discrete-Time Signals, *Philips Journal of Research,* Vol. 35, Nos. 4/5, 276-300.

8. Hlawatsch F. and Boudreaux-Bartels, G. F. (1992). Linear and quadratic time-frequency representations, *IEEE Signal Processing Magazine*, 21-67, April.

9. Chan, H. C. (1998). Detection and tracking of low-altitude aircraft using HF surface-wave radar, Defence Research Establishment Ottawa, *Report No. 1334.*

10. Chan, H. C. (1997). Iceberg detection and tracking using high frequency surface wave radar, Defence Research Establishment Ottawa, *Report No. 1310.*

UNCLASSIFIED

SECURITY CLASSIFICATION OF FORM
(highest classification of Title, Abstract, Keywords)

## DOCUMENT CONTROL DATA

(Security classification of title, body of abstract and indexing annotation must be entered when the overall document is classified)

1. ORIGINATOR (the name and address of the organization preparing the document. Organizations for whom the document was prepared, e.g. Establishment sponsoring a contractor's report, or tasking agency, are entered in section 8.)

Defence Research Establishment Ottawa
Department of National Defence
Ottawa, Ontario, Canada K1A 0Z4

2. SECURITY CLASSIFICATION (overall security classification of the document, including special warning terms if applicable)

UNCLASSIFIED

3. TITLE (the complete document title as indicated on the title page. Its classification should be indicated by the appropriate abbreviation (S,C or U) in parentheses after the title.)

Application of Wigner Distribution for the Detection of Accelerating Low-altitude Aircraft Using HF Surface-wave Radar (U)

4. AUTHORS (Last name, first name, middle initial)

Thayaparan, Thayananthan and Yasotharan, Ambighairajah

| 5. DATE OF PUBLICATION (month and year of publication of document) | 6a. NO. OF PAGES (total containing information. Include Annexes, Appendices, etc.) | 6b. NO. OF REFS (total cited in document) |
|---|---|---|
| March 2002 | 39 | 10 |

7. DESCRIPTIVE NOTES (the category of the document, e.g. technical report, technical note or memorandum. If appropriate, enter the type of report, e.g. interim, progress, summary, annual or final. Give the inclusive dates when a specific reporting period is covered.)

DREO TECHNICAL REPORT

8. SPONSORING ACTIVITY (the name of the department project office or laboratory sponsoring the research and development. Include the address.)

Defence Research Establishment Ottawa
Department of National Defence
Ottawa, Ontario, Canada K1A 0Z4

| 9a. PROJECT OR GRANT NO. (if appropriate, the applicable research and development project or grant number under which the document was written. Please specify whether project or grant) | 9b. CONTRACT NO. (if appropriate, the applicable number under which the document was written) |
|---|---|
| 05AB11 | |

| 10a. ORIGINATOR'S DOCUMENT NUMBER (the official document number by which the document is identified by the originating activity. This number must be unique to this document.) | 10b. OTHER DOCUMENT NOS. (Any other numbers which may be assigned this document either by the originator or by the sponsor) |
|---|---|
| DREO TR 2002-033 | |

11. DOCUMENT AVAILABILITY (any limitations on further dissemination of the document, other than those imposed by security classification)

(X) Unlimited distribution
( ) Distribution limited to defence departments and defence contractors; further distribution only as approved
( ) Distribution limited to defence departments and Canadian defence contractors; further distribution only as approved
( ) Distribution limited to government departments and agencies; further distribution only as approved
( ) Distribution limited to defence departments; further distribution only as approved
( ) Other (please specify):

12. DOCUMENT ANNOUNCEMENT (any limitation to the bibliographic announcement of this document. This will normally correspond to the Document Availability (11). However, where further distribution (beyond the audience specified in 11) is possible, a wider announcement audience may be selected.)

13. ABSTRACT ( a brief and factual summary of the document. It may also appear elsewhere in the body of the document itself. It is highly desirable that the abstract of classified documents be unclassified. Each paragraph of the abstract shall begin with an indication of the security classification of the information in the paragraph (unless the document itself is unclassified) represented as (S), (C), or (U). It is not necessary to include here abstracts in both official languages unless the text is bilingual).

(U) Real radar data has been analysed using the Fourier transform method and the type-III Wigner distribution. The results show that whenever the target was detectable by the Fourier transform method, the target was detectable also by the smoothed type-III Wigner distribution method. In the other trials the target was not detectable by the Fourier transform method but the target was detectable by the smoothed type-III Wigner distribution method to varying degrees of success. Based on the analysis of real radar data, we conclude that the smoothed type-III Wigner distribution provides a promising method of detecting accelerating targets. However, more work has to be done to find an optimum smoothing method. It may turn out that different smoothing methods have to be used depending on the acceleration and the closeness of the target to the clutter region. Another important contribution of the present work is the use of the type-III Wigner distribution rather than the type-I Wigner distribution which has been used by many other researchers.

When the type-I Wigner distribution is used, the range of unambiguously measurable normalized velocities is $\pi$. Moreover, targets that are $\pi$ radians away from the clutter region in the spectral domain will get masked by the clutter and cannot be detected. The type-III Wigner distribution helps us to overcome these problems. When the type-III Wigner distribution is used, the range of unambiguously measurable normalized velocities is $2\pi$, and target that are $\pi$ radians away from the clutter region can be detected.

14. KEYWORDS, DESCRIPTORS or IDENTIFIERS (technically meaningful terms or short phrases that characterize a document and could be helpful in cataloguing the document. They should be selected so that no security classification is required. Identifiers such as equipment model designation, trade name, military project code name, geographic location may also be included. If possible keywords should be selected from a published thesaurus. e.g. Thesaurus of Engineering and Scientific Terms (TEST) and that thesaurus-identified. If it is not possible to select indexing terms which are Unclassified, the classification of each should be indicated as with the title.)

Time-Frequency Analysis
Discrete-time signal
Wigner Distribution
Generalized Likelihood Ratio Test
Fourier Transform
Radon Transform
Instantaneous Frequency
High-Frequency Radar
Doppler Processing
Accelerating Targets
Doppler Radar
Doppler Smearing
Generalized Velocity
Generalized Acceleration

**Defence R&D Canada**
is the national authority for providing
Science and Technology (S&T) leadership
in the advancement and maintenance
of Canada's defence capabilities.

**R et D pour la défense Canada**
est responsable, au niveau national, pour
les sciences et la technologie (S et T)
au service de l'avancement et du maintien des
capacités de défense du Canada.


**www.drdc-rddc.dnd.ca**